Interaction between two spherical particles in a nematic liquid crystal

Jun-ichi Fukuda,[1,*] Holger Stark,[2] Makoto Yoneya,[1] and Hiroshi Yokoyama[1,3]
[1]*Yokoyama Nano-structured Liquid Crystal Project, ERATO, Japan Science and Technology Agency, 5-9-9 Tokodai, Tsukuba 300-2635, Japan*
[2]*Fachbereich Physik, Universität Konstanz, D-78457 Konstanz, Germany*
[3]*Nanotechnology Research Institute, AIST, 1-1-1 Umezono, Tsukuba 305-8568, Japan*
(Received 28 November 2003; published 30 April 2004)

We numerically investigate the interaction between two spherical particles in a nematic liquid crystal mediated by elastic distortions in the orientational order. We pay attention to the cases where two particles with equal radii R_0 impose rigid normal anchoring on their surfaces and carry a pointlike topological defect referred to as a hyperbolic hedgehog. To describe the geometry of our system, we use bispherical coordinates, which prove useful in the implementation of boundary conditions at the particle surfaces and at infinity. We adopt the Landau–de Gennes continuum theory in terms of a second-rank tensor order parameter Q_{ij} for the description of the orientational order of a nematic liquid crystal. We also utilize an adaptive mesh refinement scheme that has proven to be an efficient way of dealing with topological defects whose core size is much smaller than the particle size. When the two "dipoles," composed of a particle and a hyperbolic hedgehog, are in parallel directions, the two-particle interaction potential is attractive for large interparticle distances D and proportional to D^{-3} as expected from the form of the dipole-dipole interaction, until the well-defined potential minimum at $D \simeq 2.46R_0$ is reached. For the antiparallel configuration with no hedgehogs between the two particles, the interaction potential is repulsive and behaves as D^{-2} for $D \lesssim 10R_0$, which is stronger than the dipole-dipole repulsion ($\sim D^{-3}$) expected theoretically as an asymptotic behavior for large D.

DOI: 10.1103/PhysRevE.69.041706 PACS number(s): 61.30.Cz, 61.30.Jf, 82.70.Dd, 82.20.Wt

I. INTRODUCTION

Colloidal dispersions [1] can be found and are extensively used in our daily life such as foods, paints, and drugs. They are therefore of technological importance and one of the important subjects of fundamental science as well. Colloidal particles are either flocculated or uniformly dispersed in a host fluid, depending on the interaction between particles or droplets. Since for practical use, the properties of colloidal dispersions crucially depend on the collective behavior of the suspended particles or dispersed droplets, it is quite important to understand the two-particle interactions in a colloidal dispersion. The already known colloidal interactions include van der Waals, electrostatic, depletion [1,2] and fluctuation-induced forces [3].

Recently, colloidal dispersions in anisotropic host fluids such as liquid crystals [4–17] have been attracting growing interest as a different class of composite materials compared to conventional colloids with isotropic hosts. One of the interesting and important features of such liquid crystal colloidal dispersions is that elastic distortions of the host liquid crystal can mediate a long-range interaction between particles immersed in it [18–39], which is different in the sense that such interactions are absent in usual colloidal dispersions with isotropic host fluids. The elastic distortions of the host liquid crystal arise from the anchoring of the mesogenic molecules on the surfaces of the dispersed particles or droplets, and the resulting interaction forces mediated by the liquid crystal can be measured directly in experiments [18,19]. The long-range nature of the interaction is attributed to the fact that some of the elastic modes in liquid crystals are massless or of Goldstone type, and many analytical studies concerning the interaction between particles in a liquid crystal have been carried out so far [20–32]. In the case of a nematic liquid crystal, Lopatnikov and Namiot [20] pointed out the possibility of dipole-dipole particle interactions, i.e., the two-particle potential is anisotropic and proportional to D^{-3} with D being the interparticle distance. Later, Ramaswamy *et al.* [21] and Ruhwandl and Terentjev [22] found that the interaction between spherical particles with weak surface anchoring is quadrupolar with the potential being proportional to D^{-5}. Lubensky *et al.* [23] showed by a phenomenological argument that particles carrying a topological defect called a hyperbolic hedgehog [5,6] act as a "dipole" and the long-range interaction between them is of the same form as found by Lopatnikov and Namiot [20] mentioned above. Lev and co-workers [24] stressed that the symmetry of the particle shape serves as a crucial factor determining the type of the long-range interaction. The effect of confinement and confinement-induced director distortions has also been investigated [25]. Other types of liquid crystal phases such as smectic [26–28], columnar [29], and cholesteric [30] phases or the surface-induced paranematic order above the isotropic-nematic phase transition [31–33] have also been considered as source for interactions induced by the host fluid.

There can be another type of two-particle interaction in a liquid crystal; a short-range repulsion due to the presence of topological defects situated between the particles. When the surface anchoring and the resultant elastic distortions in a

*Electronic address: fukuda@nanolc.jst.go.jp

nematic liquid crystal are strong enough, the dispersed particles can carry topological defects in the surrounding director field such as a pointlike defect referred to as a hyperbolic hedgehog [5,6], a Saturn ring that encircles a particle as the name implies [9,40], and two surface defects called boojums [6]. Topological defects have been one of the important subjects of condensed matter physics [41–46] and liquid crystals have been known as one of the best systems where they can be observed [46–49]. Topological defects arising in liquid crystals in response to foreign inclusions provide an interesting problem on its own, and extensive theoretical [23,50–54] and numerical [33,55–66] studies have been devoted to the understanding of the profiles of the liquid crystal orientation and the topological defects close to spherical or cylindrical inclusions. Poulin and co-workers [5–7,12] argued that the long-range attraction between particle-hedgehog dipoles [23,24] and the above-mentioned short-range repulsion due to topological defects are responsible for the chainlike superstructure of the dispersed droplets with well-defined interparticle distances.

The elastic-distortion-mediated particle interactions bring about various types of superstructures, not only the linear chains [5–7,12,15] as mentioned above but also anisotropic clusters [4,8,9], periodic lattices [14,15], cellular structures [11], and the fingerprint textures that mimic those of cholesteric liquid crystals [16]. Therefore, a detailed investigation of the two-particle interactions in a liquid crystal is crucially important for the understanding of the mechanism underlying the formation of such superstructures. In spite of the wealth of analytical studies mentioned above that elucidate the properties of the particle interactions, the validity of the analytical arguments is somewhat limited because of the intrinsic difficulties in the treatment of the elasticity of liquid crystals, such as the nonlinear nature of the elastic energy or the presence of topological defects. Most of the previous analytical studies implicitly or explicitly assume either that the surface anchoring and the resultant elastic distortions in the host liquid crystal are weak enough to use a harmonic form of the elastic energy, or that the interparticle distance is much larger than the typical particle dimension. Therefore numerical calculations are inevitable for a detailed investigation of the two-particle interaction in a liquid crystal, in particular in the cases where the interparticle distance is small or where topological defects are present. There have been only a few numerical investigations for this subject. One of the first numerical studies was carried out by Stark and coworkers [33,34], who used a finite-element method together with a continuum description of the orientational order in terms of the director $\boldsymbol{n}$ to discuss the interaction between two spherical particles in a nematic droplet. Similar studies have also been performed by Patrício and co-workers [35,36] and Grollau *et al.* [37], who focused on the interaction between circular inclusions in a two-dimensional smectic-*C* [35] or nematic [36,37] liquid crystal. Very recently, molecular-dynamics simulations were carried out to calculate the interaction between infinitely long parallel cylinders in a nematic liquid crystal and the results were compared with those using a continuum theory [38]. Guzmán argued in a recent paper [66] that between two particles carrying a Saturn ring, a third disclination ring appears at short separations, which gives rise to an effective binding of the particles.

The aim of the present paper is to investigate the interaction between two spherical particles in a uniformly aligned nematic liquid crystal numerically. To describe the geometry of the two-particle system, we employ bispherical coordinates [39,67,68], while the previous numerical studies on the basis of continuum theory used triangular grids to construct the surfaces of the particles properly [33–36], or simple regular square grids without taking any special care of the curvature of the particle surfaces [37]. One of the great advantages of using bispherical coordinates is that the infinite region outside the two spheres can be mapped onto a finite rectangular region under a simple transformation. Furthermore, the bispherical coordinate system makes the treatment of the differential equations governing the elasticity of the liquid crystal and the boundary conditions both at the particle surfaces and at infinity much easier, more natural, and less computationally demanding compared to triangular or regular grids. Due to the presence of topological defects, whose core size is much smaller than the particle radii, a numerical investigation of liquid crystal colloidal dispersions becomes quite difficult. However, as has already been shown in our previous studies [39,59–63] and the work of Patrício and co-workers [35,36], the use of an adaptive mesh refinement scheme enables one to avoid those numerical difficulties. We employ the Landau–de Gennes theory of a nematic liquid crystal in terms of the second-rank tensor order parameter Q_{ij} [39,48,59–63] that allows one to describe topological defects without introducing any singularities that are inevitable in the director description in terms of the unit vector $\boldsymbol{n}$. We focus on the case where two spherical particles are accompanied by hyperbolic hedgehogs; a situation which is similar to the experiments by Poulin and co-workers [5–7,12]. To the best of our knowledge, the only previous study giving quantitative results of the interaction between (three-dimensional) spherical particles is that of Stark *et al.* [33,34]. However, their boundary conditions are different from ours since they imposed radial rather than uniform orientation at the outer boundary. Other studies [35–38] deal with essentially two-dimensional systems. Therefore we emphasize that this paper presents the three-dimensional numerical study of the interaction between spherical particles in a uniformly aligned nematic liquid crystal.

We describe our numerical system in Sec. II. In Sec. III A we present our results for the dipoles composed of a particle and a hyperbolic hedgehog in parallel directions, which is similar to the configuration found in the experiments of Poulin and co-workers [5–7,12]. In Sec. III B we deal with dipoles taking antiparallel directions with no hedgehogs between the particles. In the latter case the particles experience a repulsive interaction. We conclude this paper in Sec. IV.

II. MODEL

A. Order parameter, free energy, and the boundary conditions

For the description of the orientational order of a nematic liquid crystal, we use a second-rank traceless tensor Q_{ij} as in our previous studies [39,59–63] instead of the director $\boldsymbol{n}$ that is a unit vector and that was employed in some of the previous numerical studies concerning nematic emulsions

[33–35,55,56,65]. We notice that by using the tensor order parameter Q_{ij}, we do not have to deal with the cores of topological defects as singularities in contrast to the director description. Moreover, the tensor order parameter is consistent with the mesoscopic symmetry of the nematic liquid crystal, the equivalence of the head and tail (or $\boldsymbol{n}$ and $-\boldsymbol{n}$), and therefore can describe all of the topological defects appearing in a nematic liquid crystal, including those with half-integer strength.

The free energy of the host nematic liquid crystal in terms of Q_{ij} is written as

$$F = \int_\Omega d\boldsymbol{r}\left[\frac{1}{2}A\mathrm{Tr}\mathbf{Q}^2 - \frac{1}{3}B\mathrm{Tr}\mathbf{Q}^3 + \frac{1}{4}C(\mathrm{Tr}\mathbf{Q}^2)^2 + \frac{1}{2}L_1\partial_k Q_{ij}\partial_k Q_{ij}\right], \quad (1)$$

where Ω is the volume occupied by the nematic liquid crystal, or the region outside the two particles. The first three terms represent the bulk energy in terms of the Landau–de Gennes expansion with $\mathrm{Tr}\mathbf{Q}^2 = Q_{ij}Q_{ji}$ and $\mathrm{Tr}\mathbf{Q}^3 = Q_{ij}Q_{jk}Q_{ki}$. The indices i,j, and k denote the Cartesian coordinates x,y, and z and summations over repeated indices are implied. The coefficient C must be positive for Q_{ij} to be finite and well defined. We also notice that when $A<0$ and $B>0$, a uniaxial orientational configuration $Q_{ij} = Q[n_i n_j - (1/3)\delta_{ij}]$ minimizes the bulk energy, with $\boldsymbol{n}$ being a unit vector corresponding to the director and $Q>0$ being the scalar order parameter representing the strength of the orientational order. The last term of Eq. (1) is the elastic energy with L_1 being the elastic constant. We adopt the simplified one-constant form of the elastic energy, i.e., another term allowed from symmetry, $L_2\partial_i Q_{ij}\partial_k Q_{kj}$, is not taken into account.

Since there are many material parameters, it is convenient in the following discussion to rescale the order parameter as $Q_{ij} = s\overline{Q_{ij}}$ with $s = 2\sqrt{6}B/9C$. The free energy (1) then reads, in terms of $\overline{Q_{ij}}$,

$$\frac{F}{Cs^4} = \int_\Omega d\boldsymbol{r}\left[\frac{1}{2}\tau\mathrm{Tr}\overline{\mathbf{Q}^2} - \frac{\sqrt{6}}{4}\mathrm{Tr}\overline{\mathbf{Q}^3} + \frac{1}{4}(\mathrm{Tr}\overline{\mathbf{Q}^2})^2 + \frac{1}{2}\xi_R^2\partial_k\overline{Q_{ij}}\partial_k\overline{Q_{ij}}\right], \quad (2)$$

where $\tau \equiv A/Cs^2 = 27AC/8B^2$ is the reduced temperature, and we define the nematic coherence length as $\xi_R \equiv \sqrt{L_1/Cs^2} = \sqrt{27L_1C/8B^2}$. We notice that the first-order nematic-isotropic transition occurs at $\tau = 1/8$ and an isotropic phase becomes unstable when $\tau<0$. In what follows we omit the overbar of $\overline{Q_{ij}}$ unless confusions occur. In the simulations presented below, we are only interested in the nematic phase and set $\tau = (3\sqrt{6}-8)/12 < 0$, where $Q_{ij} = Q_{\mathrm{bulk}}[n_i n_j - (1/3)\delta_{ij}]$ with $Q_{\mathrm{bulk}} = 1$ minimizes the bulk energy.

We impose rigid homeotropic anchoring at the surfaces of two particles and fix the order parameter as $Q_{ij} = Q_s[\nu_i\nu_j - (1/3)\delta_{ij}]$, where $\boldsymbol{\nu}$ is a unit vector normal to the particle surfaces and Q_s is the scalar order parameter at the surfaces, which we will set equal to $Q_{\mathrm{bulk}} = 1$. We notice that since the order parameter at the surfaces is fixed, the particle surfaces do not contribute to the free energy of the system; therefore Eq. (2) constitutes the total free energy of the system.

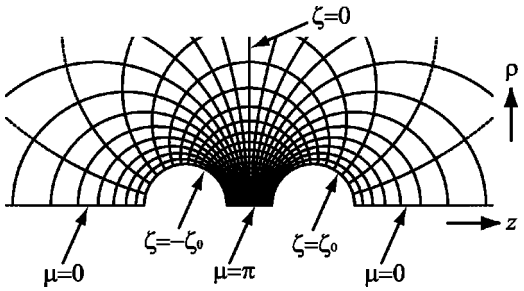

FIG. 1. Illustration of a typical mesh in real space generated by an equally spaced mesh in the (ζ,μ) space.

At infinity, we assume uniform alignment along the z axis and set $Q_{ij} = Q_{\mathrm{bulk}}[e_i^z e_j^z - (1/3)\delta_{ij}] = Q_{\mathrm{bulk}}[\delta_{iz}\delta_{jz} - (1/3)\delta_{ij}]$, where e^z is a unit vector along the z direction. This setup corresponds to placing particles with rigid homeotropic surface anchoring in a uniformly aligned nematic liquid crystal.

B. Description of the geometry and the numerical grid

We consider the case where two spherical particles with equal radii R_0 are placed in an infinite nematic medium and where the centers of the particles lie on the z axis. We denote the distance between the centers of the particles by $D(>2R_0)$ and the centers of the two particles are located at $z = \pm D/2$. For the description of the geometry of two nonintersecting particles, bispherical coordinates have proven quite useful and practical [39,67,68]. The relation between the usual cylindrical coordinates (ρ,z,ϕ) and the bispherical coordinates (ζ,μ,φ) is written as

$$\rho = \frac{a\sin\mu}{\cosh\zeta - \cos\mu}, \quad z = \frac{a\sinh\zeta}{\cosh\zeta - \cos\mu}, \quad \phi = \varphi, \quad (3)$$

where $a = \sqrt{(D/2)^2 - R_0^2}$ in our setup. The surfaces of two spheres are simply represented by $\zeta = \pm\zeta_0$ with $\zeta_0 = \cosh^{-1}(D/2R_0)$. The region outside the spheres is mapped onto a rectangle in the (ζ,μ) space given by $-\zeta_0 < \zeta < \zeta_0$ and $0 \leqslant \mu \leqslant \pi$, where $\zeta = \mu = 0$ corresponds to infinity. The z axis is represented by $\mu = 0$ or π and the plane $\zeta = 0$ in (ζ,μ) space corresponds to $z = 0$ in real space. The geometry of a typical mesh generated by an equally spaced mesh in the (ζ,μ) space is illustrated in Fig. 1. Note that although we deal with simple cases of spherical particles with equal radii, one can treat more general geometries such as two spheres with unequal radii, one sphere and a planar wall, or one sphere inside a larger sphere by appropriately choosing the upper and lower bounds of ζ.

The grids with equal spacings in the μ direction give unequal spacing on the particle surfaces in the real (ρ,z) space as can be seen in Fig. 1. Therefore, following Ref. [68], we introduce an additional variable θ as a function of μ which

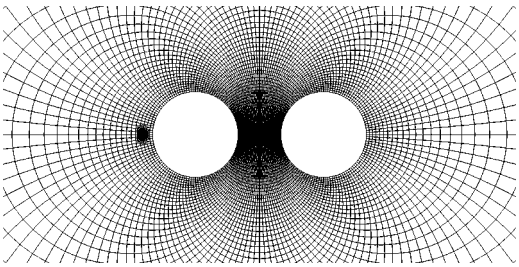

FIG. 2. The numerical grids in the real space in the case of Fig. 3(b) below.

serves as the local polar angle on the right-hand-side sphere and satisfies

$$\rho = R_0 \sin\theta, \quad z = \tfrac{1}{2}D + R_0 \cos\theta \tag{4}$$

at the surface of the right-hand-side sphere. From Eqs. (3) and (4), the relation between μ and θ is straightforward:

$$\theta = \sin^{-1}\left(\frac{a \sin\mu}{R_0(\cosh\zeta_0 - \cos\mu)}\right),$$

$$\mu = \cos^{-1}\left(\cosh\zeta_0 - \frac{a \sinh\zeta_0}{\frac{1}{2}D + R_0\cos\theta}\right). \tag{5}$$

In our calculations, we first prepare a rectangular mesh composed of 65×65 grid points with equal grid spacings in the (ζ,θ) space. Since as noted in the Introduction we are interested in the situations where topological defects are present, the numerical resolution of the mesh prepared as above may not be sufficiently high for the description of the topological defect cores. Therefore, as in our previous studies [39,59–63] we employ an adaptive mesh refinement scheme, where in the course of the relaxation of the order parameter described below, finer grids are generated by bisections in the (ζ,θ) space around the topological defect cores with strong spatial variation of the order parameter Q_{ij}. In Fig. 2, we show one of the typical numerical meshes in our calculations corresponding to Fig. 3(b) below. The grids are equally spaced at the particle surfaces and finer grids are generated around the cores of the topological defects.

For simplicity, we assume rotational symmetry about the z axis, which renders our numerical problem an effectively two-dimensional one. Since the z direction is parallel to the orientation of the nematic liquid crystal at infinity, as prescribed in Sec. II A, this assumption leads to the situations where two particles are located along the orientation of the nematic at infinity. The treatment of the order parameter is the same as that in our previous study [60,63], where the order parameter at a certain azimuthal angle ϕ is expressed by $Q_{ij}(\rho,z,\phi)=T_{ik}(\phi)T_{jl}(\phi)Q_{kl}(\rho,z,\phi=0)$, with $T_{ik}(\phi)$ being the operator of rotation by an angle ϕ whose explicit form is given in Ref. [63]. The properties of the order parameter on the symmetry axis are also essentially the same as those in Ref. [63]; $Q_{ij}=0$ when $i\neq j$ and $Q_{xx}=Q_{yy}$. Due to $\mathrm{Tr}\mathbf{Q}=0$, Q_{zz} is the only independent component of the order parameter on the symmetry axis.

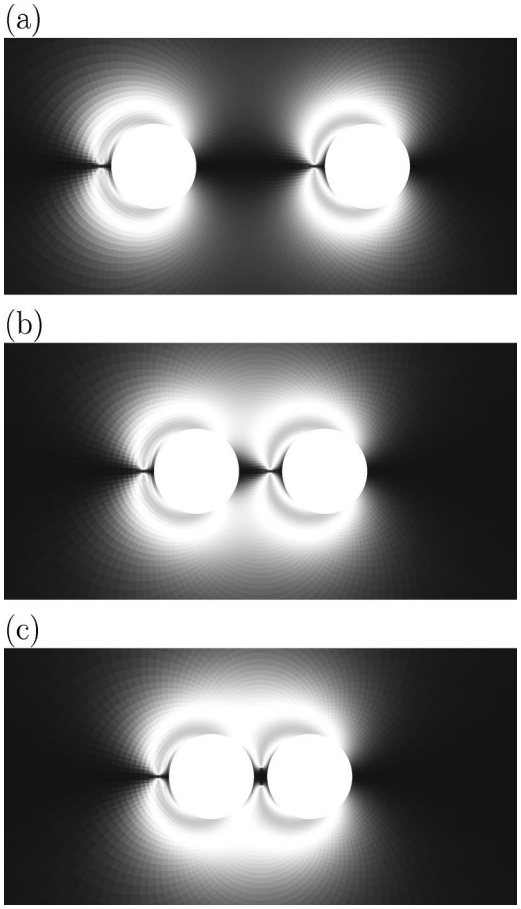

FIG. 3. The orientation profiles of a nematic liquid crystal shown by gray-scale plots of Q_{zz}^2 for (a) $D=5.0R_0$, (b) $D=3.0R_0$, and (c) $D=2.3R_0$ in the "parallel-dipole" configurations. The z axis is along the horizontal direction and in the black regions, the nematic liquid crystal aligns along the z axis, while $Q_{zz}=0$ in the white region.

C. Evaluation of the free energy

From Eq. (3), it can be shown that the Jacobian $\partial(x,y,z)/\partial(\zeta,\mu,\phi)$ is equal to $a^3\sin\mu/(\cosh\zeta-\cos\mu)^3$. Moreover, keeping in mind the choice $\tau=(3\sqrt{6}-8)/12$ in Sec. II A and $Q_{ij}=Q_{\mathrm{bulk}}[n_in_j-(1/3)\delta_{ij}]$ with $Q_{\mathrm{bulk}}=1$ minimizing the bulk energy, we find that the free energy density of a uniform undistorted nematic liquid crystal is $-(4-\sqrt{6})/36$. Therefore from Eq. (2) the (dimensionless) free energy of a nematic liquid crystal due to the elastic distortion by the particles reads

$$\begin{aligned}\overline{F} &= \frac{F}{Cs^4R_0^3} \\ &= 2\pi\int_{-\zeta_0}^{\zeta_0} d\zeta \int_0^{\pi} d\mu \left(\frac{a}{R_0}\right)^3 \frac{\sin\mu}{(\cosh\zeta-\cos\mu)^3}\left[\frac{1}{2}\tau\mathrm{Tr}\mathbf{Q}^2\right. \\ &\quad \left. -\frac{\sqrt{6}}{4}\mathrm{Tr}\mathbf{Q}^3+\frac{1}{4}\mathrm{Tr}\mathbf{Q}^4+\frac{4-\sqrt{6}}{36}+\frac{1}{2}\overline{\xi_R^2}\overline{\partial}_k Q_{ij}\overline{\partial}_k Q_{ij}\right],\end{aligned} \tag{6}$$

where the factor 2π is due to the rotational symmetry about

the z axis. We have also defined the reduced nematic coherence length $\bar{\xi}_R=\xi_R/R_0$ and the spatial derivative $\bar{\partial}_k=R_0\partial_k$. We evaluate the discretized version of Eq. (6) using the trapezoidal rule [69] generalized to the two-dimensional (ζ,μ) space as in our previous study [63]. For the evaluation of the first-order derivatives $\partial_k Q_{ij}$, see the Appendix.

D. Relaxation of the order parameter

To obtain the equilibrium profiles of the orientational order parameter Q_{ij} for a given interparticle distance D, we first prepare an initial configuration and let it relax via a simple equation of motion for Q_{ij}:

$$\frac{\partial}{\partial t}Q_{ij}(\mathbf{r}) = -\Gamma\left(\frac{\delta F}{\delta Q_{ij}(r)}+\lambda\delta_{ij}\right) = -\Gamma\left(\tau Q_{ij}-\frac{3\sqrt{6}}{4}Q_{ik}Q_{kj}+\mathrm{Tr}\mathsf{Q}^2Q_{ij} - \xi_R^2\nabla^2 Q_{ij}+\lambda\delta_{ij}\right), \tag{7}$$

which is referred to as model A in the notation of Hohenberg and Halperin [70]. Here Γ is a kinetic coefficient inversely proportional to the rotational viscosity and λ is a Lagrange multiplier ensuring $\mathrm{Tr}\mathsf{Q}=0$. In the bispherical coordinates, the Laplacian ∇^2 is given by

$$\nabla^2=\frac{(\cosh\zeta-\cos\mu)}{a^2}\left\{(\cosh\zeta-\cos\mu)\left[\frac{\partial^2}{\partial\zeta^2}+\frac{\partial^2}{\partial\mu^2}+\frac{1}{\sin^2\mu}\frac{\partial^2}{\partial\phi^2}\right]-\sinh\zeta\frac{\partial}{\partial\zeta}-\frac{(1-\cosh\zeta\cos\mu)}{\sin\mu}\frac{\partial}{\partial\mu}\right\}. \tag{8}$$

The numerical evaluation of the first and second-order derivatives appearing in Eq. (8) is carried out using the same technique as in our previous study, whose detail is presented in Ref. [63].

On the axis of rotational symmetry (z axis, $\sin\mu=0$), the only independent component of $\nabla^2 Q_{ij}$ is $\nabla^2 Q_{zz}$, because $\nabla^2 Q_{xx}=\nabla^2 Q_{yy}=-(1/2)\nabla^2 Q_{zz}$ and $\nabla^2 Q_{ij}=0$ for $i\neq j$ [63]. For the calculation of $\nabla^2 Q_{zz}$, the argument presented in Ref. [68] can be directly used and we obtain

$$\nabla^2 Q_{zz}|_{z\text{-axis}}=\frac{(\cosh\zeta-\cos\mu)}{a^2}\left\{(\cosh\zeta-\cos\mu)\left[\frac{\partial^2}{\partial\zeta^2}+2\frac{\partial^2}{\partial\mu^2}\right]-\sinh\zeta\frac{\partial}{\partial\zeta}\right\}Q_{zz}. \tag{9}$$

As the initial condition, we set the order parameter at the point $\boldsymbol{r}$ to $Q_{ij}(\boldsymbol{r})=Q_{\mathrm{bulk}}[n_i(\boldsymbol{r})n_j(\boldsymbol{r})-(1/3)\delta_{ij}]$ with $Q_{\mathrm{bulk}}=1$ in the bulk and $Q_{ij}(\boldsymbol{r})=0$ close to the initial position of the topological defect cores. We follow the spirit of Ref. [23] and choose the director $\boldsymbol{n}(\boldsymbol{r})$ as $\boldsymbol{n}(\boldsymbol{r})\cdot\boldsymbol{e}^z=\cos\Theta(\boldsymbol{r})$, $\boldsymbol{n}(\boldsymbol{r})\cdot\boldsymbol{e}^\rho=\sin\Theta(\boldsymbol{r})$ and $\boldsymbol{n}(\boldsymbol{r})\cdot\boldsymbol{e}^\phi=0$, where $\boldsymbol{e}^z$, $\boldsymbol{e}^\rho$, and $\boldsymbol{e}^\phi$ are the unit vectors in the cylindrical coordinates and

$$\Theta(\boldsymbol{r})=\sum_{i=1,2}\left(2\tan^{-1}\frac{\rho}{z-z_{Si}}-\frac{1}{2}\left[\tan^{-1}\frac{\rho-(R_0^2/r_{di})\sin\theta_{di}}{z-[z_{Si}+(R_0^2/r_{di})\cos\theta_{di}]}+\tan^{-1}\frac{\rho+(R_0^2/r_{di})\sin\theta_{di}}{z-[z_{Si}+(R_0^2/r_{di})\cos\theta_{di}]}+\tan^{-1}\frac{\rho-r_{di}\sin\theta_{di}}{z-(z_{Si}+r_{di}\cos\theta_{di})}\right.\right.$$
$$\left.+\tan^{-1}\frac{\rho+r_{di}\sin\theta_{di}}{z-(z_{Si}+r_{di}\cos\theta_{di})}\right]+e^{-k/r_i^3}\left\{\left(\frac{r_{di}}{R_0}+\frac{R_0}{r_{di}}\right)\left[\frac{R_0}{r_i}-\left(\frac{R_0}{r_i}\right)^2\right]\frac{\rho}{r_i}\cos\theta_{di}+\left[\left(\frac{r_{di}}{R_0}\right)^2+\left(\frac{R_0}{r_{di}}\right)^2\right]\right.$$
$$\times\left[\left(\frac{R_0}{r_i}\right)^2-\left(\frac{R_0}{r_i}\right)^3\right]\frac{\rho(z-z_{Si})}{r_i^2}(2\cos^2\theta_{di}-1)+\frac{1}{3}\left[\left(\frac{r_{di}}{R_0}\right)^3+\left(\frac{R_0}{r_{di}}\right)^3\right]\left[\left(\frac{R_0}{r_i}\right)^3-\left(\frac{R_0}{r_i}\right)^4\right]\frac{\rho}{r_i}\left[4\left(\frac{z-z_{Si}}{r_i}\right)^2-1\right]$$
$$\left.\left.\times\cos\theta_{di}(4\cos^2\theta_{di}-3)\right\}\right). \tag{10}$$

Equation (10) is just the superposition of the "ansatz" configurations of the disclination rings given in Eq. (33) of Ref. [23]. $z_{Si}=(-1)^{i+1}D/2$ is the z coordinate of the center of the ith spherical particle with $i=1$ or 2, and $r_i=\sqrt{\rho^2+(z-z_{Si})^2}$ is the distance of the point $\boldsymbol{r}$ from the center of the ith particle. r_{di} and θ_{di} with $i=1,2$ specify the position of the two disclination rings and the position of their cores is $z=z_{Si}+r_{di}\cos\theta_{di}$, $\rho=r_{di}\sin\theta_{di}$. We set the variational parameter k to 0.32 as in Ref. [23]. We notice that $\theta_{di}=0$ or π corresponds to considering a hyperbolic hedgehog point defect and $\theta_{di}=\pi/2$ a Saturn ring. However, in our previous studies [60,71] we found that a hyperbolic hedgehog defect takes a structure of a small ring rather than a point. Therefore, keeping this finding in mind, we choose $\theta_{di}=(1/90)\pi$ or $(1-1/90)\pi$ depending on the configurations we want to investigate (notice that in this paper we do not consider a Saturn ring). In most of our numerical calculations we set $r_{di}=1.22$ for $i=1,2$. When $D\leqslant 2.44$ and one of the hedgehog defects is located between the two particles, we use $r_{di}=D/2$ for that defect. Finally it should be noted that although Eq. (10) successfully reproduces the asymptotic behavior of the director at infinity [23], it does

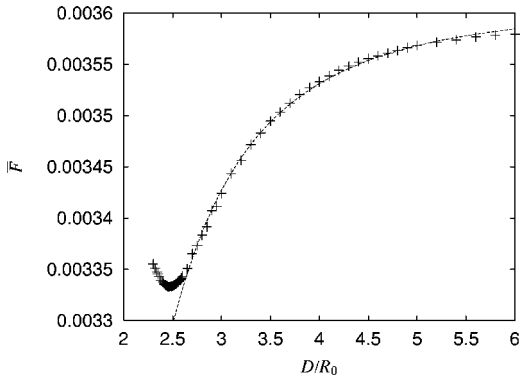

FIG. 4. The dimensionless free energy of a nematic liquid crystal $\overline{F}$ as a function of the distance D between the centers of the particles in the case of the "parallel-dipole" configuration. The inset is a magnified plot around $D/R_0=2.45$.

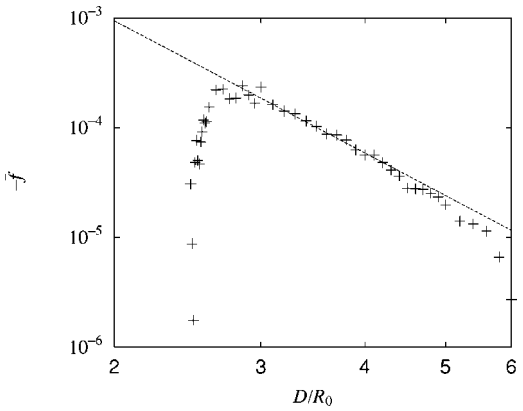

FIG. 5. Log-log plot of the dimensionless force $\overline{f}$ as a function of D in the case of the "parallel-dipole" configuration. The dashed line corresponds to $0.0150(D/R_0)^{-4}$. Only the data for the attractive force ($-\overline{f}>0$) are shown.

not satisfy the boundary conditions at the particle surfaces (rigid normal anchoring). This mismatch is reconciled by the relaxation equation (7).

III. RESULTS AND DISCUSSIONS

We first notice that in all the following simulations the dimensionless nematic coherence length is set to $\overline{\xi_R}=5\times10^{-3}$. We have checked the stability of a hedgehog configuration in the case of one particle using the same simulation scheme as in our previous study [60,63] and found that for $\overline{\xi_R}=5\times10^{-3}$ the hedgehog configuration is indeed stable (at least metastable). Using the parameters in Ref. [72], $B\simeq360$ kJ m^{-3}, $C\simeq300$ kJ m^{-3}, and $L_1/C\simeq10^4$ Å^2, we have $\xi_R\simeq15$ nm and the choice $\overline{\xi_R}=5\times10^{-3}$ corresponds to taking $R_0\simeq3$ μm.

A. Parallel dipoles

In Fig. 3 we show several typical orientation profiles for different interparticle distances D, where the particles carry a hyperbolic hedgehog defect and the orientation of the two dipoles composed of a particle and a hedgehog is parallel. This configuration is similar to a part of the experimentally observed chain-like structures in a uniformly aligned nematic liquid crystal [5–7,12]. In the initial condition presented in Eq. (10), we choose $\theta_{di}=(1-1/90)\pi$. For large D [Fig. 3(a)], the configurations of a nematic liquid crystal around each particle are almost independent and uncorrelated; they are those around an isolated particle, while for smaller D [Figs. 3(b) and 3(c)], deviations of the orientation profiles from those of two isolated particles are clearly found. Moreover, in Fig. 3(c) with $D=2.3R_0$ we also observe that the hedgehog situated between the particles opens up to form a larger ring (we notice again that the hedgehog defect originally takes the form of a small ring [60,71]). This behavior may be observed in an experiment using two optical tweezers and may provide evidence that the hedgehog indeed possesses the structure of a ring and not a point.

We plot in Fig. 4 the dimensionless free energy of the liquid crystal $\overline{F}$ defined in Eq. (6) as a function of the interparticle distance D. We notice that this free energy is the sum of the self-energies of two particles (energy of an isolated particle) and the interaction energy arising from the elastic distortion of the liquid crystal. The dashed line is $0.003\,61-0.004\,86(D/R_0)^{-3}$, which indicates that when the interparticle distance is large enough, the interaction is attractive and its potential energy is proportional to $-D^{-3}$. This corresponds to the long-range dipole-dipole interaction discussed theoretically [23,24]. We also show in Fig. 5 the log-log plot of the dimensionless force acting on one particle $\overline{f}=-R_0(d\overline{F}/dD)$ as a function of D [73]. When $-\overline{f}>0$ the force is attractive and we show in Fig. 5 only data for attractive forces. The dashed line in Fig. 5 corresponds to $0.0150(D/R_0)^{-4}$. Therefore Fig. 5 demonstrates that the long-range attractive force is proportional to D^{-4}, consistent with the above argument that the interaction potential is proportional to D^{-3}. We also notice that this D^{-4} dependence of the long-range interaction force was observed experimentally [18].

When D is small, the interaction becomes repulsive and the potential minimum is found at $D\simeq2.46R_0$. This short-range repulsion arises from the presence of the hyperbolic hedgehog defect situated between the particles and its deformation to a larger ring. The balance between the long-range dipole-dipole attraction and the short-range repulsion due to the topological defect results in the potential minimum mentioned above. This type of interaction potential is the reason for the chainlike superstructures made up of particles with well-defined interparticle distances observed experimentally [5–7,12].

B. Antiparallel dipoles

In this section we discuss the configuration where the two dipoles take antiparallel directions. We do not consider the situation where two hedgehogs lie between the two particles, because it is experimentally observed [19] that such a configuration is quite unstable and one of the particles escapes

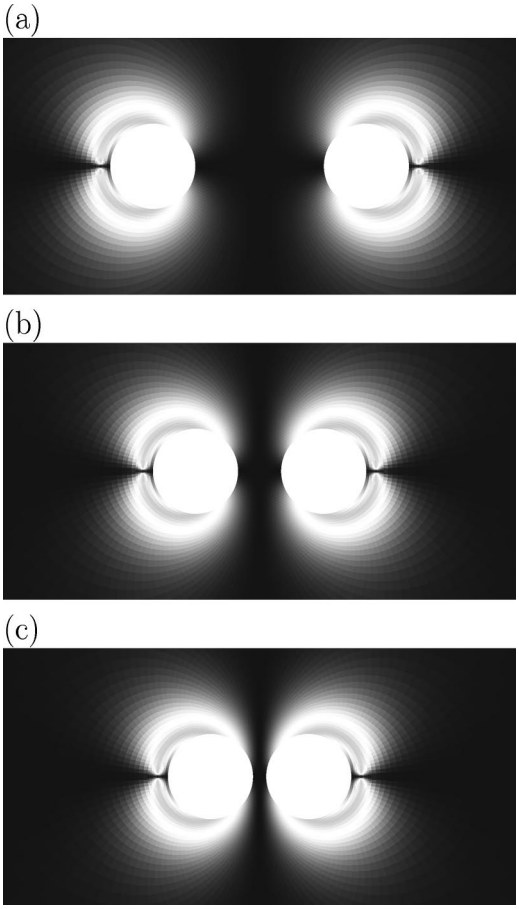

FIG. 6. The orientation profiles of a nematic liquid crystal shown by gray-scale plots of Q_{zz}^2 for (a) $D=5.0R_0$, (b) $D=3.0R_0$, and (c) $D=2.3R_0$ in the "antiparallel-dipole" configurations.

from the line along the orientation of the nematic liquid crystal at infinity, just as it is very difficult to let two bar magnets with antiparallel directions approach each other on one line. As noted in Sec. II B, in our setup the particles must lie on the z axis. Therefore, we only deal with the case where no topological defects lie between the particles. In Fig. 6 we show several typical orientation profiles for different interparticle distances D. As in the previous case for parallel dipoles, when the particle distance is large enough, the orientation profiles around each particle are almost the same as that around an isolated particle [Fig. 6(a)]. The distortions of the orientation profiles are not strong but observable in the case of smaller interparticle distances [Figs. 6(b) and 6(c)].

From the theoretical arguments in Refs. [23,24], it is expected that the two-particle interaction for antiparallel dipoles is repulsive and that its potential energy is proportional to D^{-3}. We plot in Fig. 7 the (dimensionless) free energy of the liquid crystal $\bar{F}$ as a function of the interparticle distance D. From Fig. 7 we find that the interaction is indeed repulsive, but the dashed line of Fig. 7 is given by $0.003\,55+0.001\,51(D/R_0)^{-2}$. Trials of the fitting of the numerical results by a function $a+b(D/R_0)^{-n}$ with a and b being fitting parameters and n being an integer other than 2 were not successful [when n is not restricted to an integer, the numerical data are best fitted by $0.003\,55+0.001\,79(D/R_0)^{-2.17}$. We

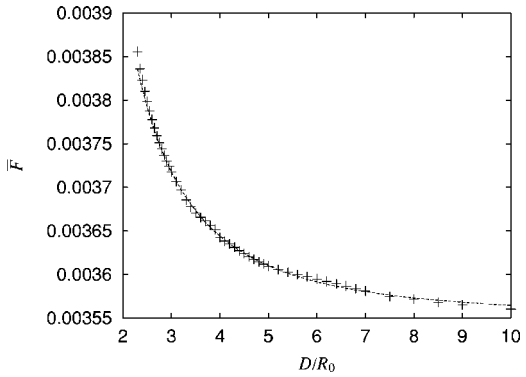

FIG. 7. The dimensionless free energy of a nematic liquid crystal $\bar{F}$ as a function of the distance D between the centers of the particles in the case of the "antiparallel-dipole" configuration.

also plot in Fig. 8 the dimensionless force $\bar{f}$ as a function of D. In this case $\bar{f}>0$, which implies that the force is repulsive. Although numerical errors are present, the data points fall well onto the dashed line, $0.003\,45(D/R_0)^{-3}\propto D^{-3}$, which also supports the above finding that the interaction potential is proportional to D^{-2}.

To our knowledge, such a repulsive interaction whose potential is proportional to D^{-2} has never been found in any previous analytic and numerical studies concerning the interaction between particles in a liquid crystal. As was emphasized in the Introduction, almost all of the previous analytic studies implicitly assume that the interparticle distance is much larger than the dimension of the particles, therefore our present result may reveal the limitation of the validity of the analytic studies in the case of medium interparticle distances. Although a clear theoretical interpretation of our results is not available so far, the particles can be regarded as radial hedgehogs, and the bare repulsion between those two radial hedgehogs may render the interaction in the present case stronger than the dipole-dipole one.

We notice that the present case with antiparallel dipoles has never been discussed in any previous numerical or experimental studies, so the comparison between our results

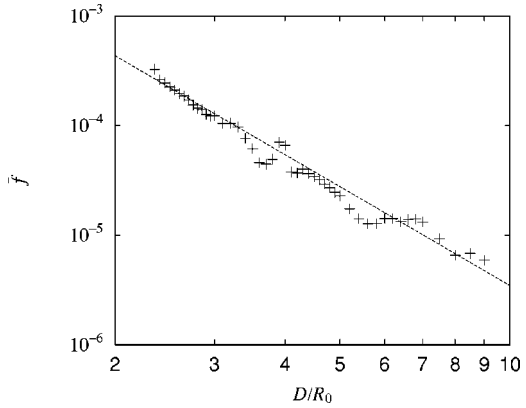

FIG. 8. Log-log plot of the dimensionless force $\bar{f}$ as a function of D in the case of the "antiparallel-dipole" configuration. The dashed line corresponds to $0.003\,45\ (D/R_0)^{-3}$.

and previous numerical or experimental ones cannot be done. Therefore we hope that our results will promote further experiments concerning the interaction between particles in a nematic liquid crystal. Finally, note that the antiparallel-dipole configuration possesses a mirror symmetry about the $z=0$ plane that lies between the particles. We therefore conclude that the interaction of a particle, carrying a hyperbolic hedgehog, and a planar wall, imposing strong homeotropic anchoring, should show the same behavior as our results.

IV. CONCLUSION

We numerically investigated the interaction mediated by the elastic distortions of a nematic liquid crystal between two spherical particles imposing a rigid homeotropic anchoring and carrying a hyperbolic hedgehog defect in a uniformly aligned nematic. We employed the Landau–de Gennes continuum theory where the orientational order of a nematic liquid crystal is described in terms of a second-rank tensor order parameter Q_{ij} and the topological defects can be treated without introducing any singularities. In contrast to similar numerical studies in which triangular grids or regular square grids were used, we utilized bispherical coordinates for the description of the geometry of the system containing two spherical particles. They enabled us to naturally implement the boundary conditions at the particle surfaces and at infinity.

We found that when the dipoles composed of a particle and a hyperbolic hedgehog defect align in parallel directions, the interaction potential is attractive for large particle separations D and behaves as D^{-3} until it reaches its minimum at $D \simeq 2.46R_0$ (R_0 is the particle radius). The long-range attraction is of dipolar type and consistent with previous experimental results and those of analytical studies. The potential minimum arises from the short-range repulsion that is attributed to the presence of a hyperbolic hedgehog defect and its elastic distortion to a larger ring. The balance between the long-range attraction and the short-range repulsion is the reason for the experimentally observed chainlike superstructure of particles with well-defined interparticle distances in a uniformly aligned nematic liquid crystal.

We also investigated the case where the two dipoles take the antiparallel configuration with no hedgehog defects situated between the two particles. The particles experience a repulsive interaction and the dependence of its potential on the interparticle distance is D^{-2}, in contrast to the "parallel dipoles" mentioned above or theoretical expectations whose potential is proportional to D^{-3}. This result may show that the validity of analytic arguments is somewhat limited because they assume that the interparticle distance is much larger than the dimension of the particle. A clear theoretical argument that explains the D^{-2} dependence is not available so far. However, the stronger dependence on D may be attributed to the bare interaction between two particles that behave as radial hedgehogs. We finally notice that there have been almost no experimental studies that focused on the repulsive interaction between particles in a nematic liquid crystal. We therefore hope that our present results will encourage further experimental as well as numerical studies concerning the elastic-distortion-mediated interactions in a liquid crystal.

ACKNOWLEDGMENT

J.F. is grateful to Dr. Makoto Yada for helpful conversations on his experiments.

APPENDIX: FIRST-ORDER DERIVATIVES

In this appendix we show how to calculate first-order derivatives necessary for the evaluation of the free energy (6). From Eq. (3) the calculation of the Jacobi matrix is straightforward and noticing that $x=\rho\cos\phi$ and $y=\rho\sin\phi$, we have

$$\begin{pmatrix} \frac{\partial}{\partial x} \\ \frac{\partial}{\partial y} \\ \frac{\partial}{\partial z} \end{pmatrix} = \begin{pmatrix} -\frac{1}{a}\sinh\zeta\sin\mu\cos\phi & \frac{1}{a}(\cosh\zeta\cos\mu-1)\cos\phi & -\frac{1}{\rho}\sin\phi \\ -\frac{1}{a}\sinh\zeta\sin\mu\sin\phi & \frac{1}{a}(\cosh\zeta\cos\mu-1)\sin\phi & \frac{1}{\rho}\cos\phi \\ \frac{1}{a}(1-\cosh\zeta\cos\mu) & -\frac{1}{a}\sinh\zeta\sin\mu & 0 \end{pmatrix} \begin{pmatrix} \frac{\partial}{\partial\zeta} \\ \frac{\partial}{\partial\mu} \\ \frac{\partial}{\partial\phi} \end{pmatrix}. \tag{A1}$$

At the axis of rotational symmetry (the z axis), care must be taken in the use of Eq. (A1) because $\rho=0$ there. There is no problem in the treatment of $\partial/\partial z$ and $\sin\mu=0$ straightforwardly yields $\partial Q_{ij}/\partial z=(1/a)(1-\cosh\zeta\cos\mu)(\partial/\partial\zeta)$ ($\cos\mu=1$ or -1). It can also be shown [63] that when rotational symmetry is assumed, $\partial Q_{ij}/\partial x=\partial Q_{ij}/\partial y=0$ for $ij=xx,yy,zz$, and xy at the symmetry axis. As for Q_{xz} (the same argument holds for Q_{yz}), we notice that it is regular

around the z axis and therefore can be expanded in terms of ρ as $Q_{xz}=Q_{xz}^{(0)}(z,\phi)+\rho Q_{xz}^{(1)}(z,\phi)+\frac{1}{2}\rho^2 Q_{xz}^{(2)}(z,\phi)+\cdots$, where we assume the regularity of $Q_{xz}^{(i)}\equiv\partial^i Q_{xz}/\partial\rho^i$. Since Q_{xz} should be independent of ϕ at the z axis, $\partial Q_{xz}^{(0)}/\partial\phi=0$. Therefore $(1/\rho)\partial Q_{xz}/\partial\phi$ is regular at the z axis. Then at the z axis $(-1/\rho)\sin\phi(\partial Q_{xz}/\partial\phi)$ and $(1/\rho)\cos\phi\partial(Q_{xz}/\partial\phi)$ can be safely set to zero at $\phi=0$ and $\phi=\pi/2$, respectively. From Eq. (A1) and $\sin\mu=0$, we finally obtain

$$\left.\frac{\partial Q_{xz}}{\partial x}\right|_{z\text{-axis}}=\frac{1}{a}(\cosh\zeta\cos\mu-1)\left.\frac{\partial Q_{xz}}{\partial\mu}\right|_{z\text{-axis},\phi=0},$$

$$\left.\frac{\partial Q_{xz}}{\partial y}\right|_{z\text{-axis}}=\frac{1}{a}(\cosh\zeta\cos\mu-1)\left.\frac{\partial Q_{xz}}{\partial\mu}\right|_{z\text{-axis},\phi=\pi/2}. \quad \text{(A2)}$$

[1] W. B. Russel, D. A. Saville, and W. R. Schowalter, *Colloidal Dispersions* (Cambridge University Press, Cambridge, 1995).

[2] J. N. Israelachvili, *Intermolecular and Surface Forces* (Academic Press, London, 1992).

[3] V. M. Mostepanenko and N. N. Trunov, *The Casimir Effect and its Application* (Clarendon Press, Oxford, 1997).

[4] P. Poulin, V. A. Raghunathan, P. Richetti, and D. Roux, J. Phys. II **4**, 1557 (1994); V. A. Raghunathan, P. Richetti, and D. Roux, Langmuir **12**, 3789 (1996); V. A. Raghunathan, P. Richetti, D. Roux, F. Nallet, and A. K. Sood, Mol. Cryst. Liq. Cryst. **288**, 181 (1996); Langmuir **16**, 4720 (2000).

[5] P. Poulin, H. Stark, T. C. Lubensky, and D. A. Weitz, Science **275**, 1770 (1997).

[6] P. Poulin and D. A. Weitz, Phys. Rev. E **57**, 626 (1998).

[7] P. Poulin, Curr. Opin. Colloid Interface Sci. **4**, 66 (1999).

[8] P. Poulin, N. Francès, and O. Mondain-Monval, Phys. Rev. E **59**, 4384 (1999).

[9] O. Mondain-Monval, J. C. Dedieu, T. Gulik-Krzywicki, and P. Poulin, Eur. Phys. J. B **12**, 167 (1999).

[10] M. Zapotocky, L. Ramos, P. Poulin, T. C. Lubensky, and D. A. Weitz, Science **283**, 209 (1999); L. Ramos, M. Zapotocky, T. C. Lubensky, and D. A. Weitz, Phys. Rev. E **66**, 031711 (2002).

[11] S. P. Meeker, W. C.K. Poon, J. Crain, and E. M. Terentjev, Phys. Rev. E **61**, R6083 (2000); V. J. Anderson, E. M. Terentjev, S. P. Meeker, J. Crain, and W. C.K. Poon, Eur. Phys. J. E **4**, 11 (2001); V. J. Anderson and E. M. Terentjev, *ibid.* **4**, 21 (2001).

[12] J.-C. Loudet, P. Barois, and P. Poulin, Nature (London) **407**, 611 (2000); J. C. Loudet, P. Poulin, and P. Barois, Europhys. Lett. **54**, 175 (2001).

[13] J. Yamamoto and H. Tanaka, Nature (London) **409**, 321 (2001).

[14] V. G. Nazarenko, A. B. Nych, and B. I. Lev, Phys. Rev. Lett. **87**, 075504 (2001).

[15] P. Cluzeau, V. Dolganov, P. Poulin, G. Joly, and H. T. Nguyen, Mol. Cryst. Liq. Cryst. **364**, 381 (2001); P. Cluzeau, P. Poulin, G. Joly, and H. T. Nguyen, Phys. Rev. E **63**, 031702 (2001); P. Cluzeau, G. Joly, H. T. Nguyen, and V. K. Dolganov, JETP Lett. **75**, 482 (2002); **76**, 351 (2002); P. Cluzeau, V. Bonnand, G. Joly, V. Dolganov, and H. T. Nguyen, Eur. Phys. J. E **10**, 231 (2003).

[16] M. Mitov, C. Portet, C. Bourgerette, E. Snoeck, and M. Verelst, Nat. Mater. **1**, 229 (2002).

[17] T. Bellini, M. Caggioni, N. A. Clark, F. Mantegazza, A. Maritan, and A. Pelizzola, Phys. Rev. Lett. **91**, 085704 (2003).

[18] P. Poulin, V. Cabuil, and D. A. Weitz, Phys. Rev. Lett. **79**, 4862 (1997).

[19] M. Yada, J. Yamamoto, and H. Yokoyama, Phys. Rev. Lett. (to be published); The Third International Symposium on Slow Dynamics in Complex Systems, Sendai, Japan, 2003, Poster Presentation C_FE-P9 (unpublished).

[20] S. L. Lopatnikov and V. A. Namiot, Zh. Eksp. Teor. Fiz. **25**, 361 (1978) [Sov. Phys. JETP **48**, 180 (1978)].

[21] S. Ramaswamy, R. Nityananda, V. A. Raghunathan, and J. Prost, Mol. Cryst. Liq. Cryst. Sci. Technol., Sect. A **288**, 175 (1996).

[22] R. W. Ruhwandl and E. M. Terentjev, Phys. Rev. E **55**, 2958 (1997).

[23] T. C. Lubensky, D. Pettey, N. Currier, and H. Stark, Phys. Rev. E **57**, 610 (1998).

[24] B. I. Lev and P. M. Tomchuk, Phys. Rev. E **59**, 591 (1999); S. B. Chernyshuk, B. I. Lev, and H. Yokoyama, Sov. Phys. JETP **93**, 760 (2001); B. I. Lev, S. B. Chernyshuk, P. M. Tomchuk, and H. Yokoyama, Phys. Rev. E **65**, 021709 (2002).

[25] J. Fukuda, B. I. Lev, K. M. Aoki, and H. Yokoyama, Phys. Rev. E **66**, 051711 (2002); Mol. Cryst. Liq. Cryst. (to be published); J. Fukuda, B. I. Lev, and H. Yokoyama, J. Phys.: Condens. Matter **15**, 3841 (2003).

[26] M. S. Turner and P. Sens, Phys. Rev. E **55**, R1275 (1997); P. Sens, M. S. Turner, and P. Pincus, *ibid.* **55**, 4394 (1997); P. Sens and M. S. Turner, J. Phys. II **7**, 1855 (1997); M. S. Turner and P. Sens, Phys. Rev. E **57**, 823 (1998).

[27] J. Groenwold and G. H. Fredrickson, Eur. Phys. J. E **5**, 171 (2001).

[28] C. D. Santangelo and R. D. Kamien, Phys. Rev. Lett. **91**, 045506 (2003).

[29] R. Adhikari, Eur. Phys. J. E **9**, 127 (2002).

[30] J. Fukuda, B. I. Lev, and H. Yokoyama, Phys. Rev. E **65**, 031710 (2002).

[31] A. Borštnik, H. Stark, and S. Žumer, Phys. Rev. E **60**, 4210 (1999); **61**, 2831 (2000).

[32] P. Galatola and J.-B. Fournier, Phys. Rev. Lett. **86**, 3915 (2001); J.-B. Fournier and P. Galatola, Phys. Rev. E **65**, 032702 (2002); H. Stark, *ibid.* **66**, 041705 (2002); P. Galatola, J.-B. Fournier, and H. Stark, *ibid.* **67**, 031404 (2003).

[33] H. Stark, Phys. Rep. **351**, 387 (2001).

[34] H. Stark, J. Stelzer, and R. Bernhard, Eur. Phys. J. B **10**, 515 (1999).

[35] P. Patrício, M. Tasinkevych, and M. M. Telo da Gama, Eur. Phys. J. E **7**, 117 (2002).

[36] M. Tasinkevych, N. M. Silvestre, P. Patrício, and M. M. Telo da Gama, Eur. Phys. J. E **9**, 341 (2002).

[37] S. Grollau, E. B. Kim, O. Guzmán, N. L. Abbott, and J. J. de

Pablo, J. Chem. Phys. **119**, 2444 (2003).
[38] D. Andrienko, M. Tasinkevych, P. Patricío, M. P. Allen, and M. M. Telo da Gama, Phys. Rev. E **68**, 051702 (2003).
[39] J. Fukuda, M. Yoneya, H. Yokoyama, and H. Stark, The Eighth IUMRS International Conference on Advanced Materials, Yokohama, Japan, 2003, Poster Presentation D11-12-P01 (unpublished); Colloids Surf., B (to be published).
[40] Y. Gu and N. L. Abbott, Phys. Rev. Lett. **85**, 4719 (2000).
[41] N. D. Mermin, Rev. Mod. Phys. **51**, 591 (1979).
[42] H.-R. Trebin, Adv. Phys. **31**, 195 (1982).
[43] M. Kléman, *Points, Lines, and Walls: in Liquid Crystals, Magnetic Systems, and Various Ordered Media* (Wiley, New York, 1983).
[44] P. M. Chaikin and T. C. Lubensky, *Principles of Condensed Matter Physics* (Cambridge University Press, Cambridge, 1995).
[45] D. R. Nelson, *Defects and Geometry in Condensed Matter Physics* (Cambridge University Press, Cambridge, 2002).
[46] M. Kleman and O. D. Lavrentovich, *Soft Matter Physics: An Introduction* (Springer-Verlag, New York, 2003).
[47] S. Chandrasekhar, *Liquid Crystals*, 2nd ed. (Cambridge University Press, Cambridge, 1992).
[48] P. G. de Gennes and J. Prost, *The Physics of Liquid Crystals*, 2nd ed. (Oxford University Press, Oxford, 1993).
[49] D. Demus and L. Richter, *Textures of Liquid Crystals* (Verlag Chemie, New York, 1978).
[50] S. V. Burylov and Y. L. Raikher, Phys. Rev. E **50**, 358 (1994).
[51] E. M. Terentjev, Phys. Rev. E **51**, 1330 (1995).
[52] O. V. Kuksenok, R. W. Ruhwandl, S. V. Shiyanovskii, and E. M. Terentjev, Phys. Rev. E **54**, 5198 (1996).
[53] S. V. Shiyanovskii and O. V. Kuksenok, Mol. Cryst. Liq. Cryst. Sci. Technol., Sect. A **321**, 45 (1998)
[54] H. Stark, Phys. Rev. E **66**, 032701 (2002).
[55] R. W. Ruhwandl and E. M. Terentjev, Phys. Rev. E **56**, 5561 (1997).
[56] H. Stark, Eur. Phys. J. B **10**, 311 (1999).
[57] J. L. Billeter and R. A. Pelcovits, Phys. Rev. E **62**, 711 (2000).
[58] D. Andrienko, G. Germano, and M. P. Allen, Phys. Rev. E **63**, 041701 (2001).
[59] J. Fukuda and H. Yokoyama, Eur. Phys. J. E **4**, 389 (2001).
[60] J. Fukuda, M. Yoneya, and H. Yokoyama, Phys. Rev. E **65**, 041709 (2002).
[61] J. Fukuda, M. Yoneya, and H. Yokoyama, Mol. Cryst. Liq. Cryst. (to be published).
[62] J. Fukuda, H. Stark, M. Yoneya, and H. Yokoyama, J. Phys.: Condens. Matter (to be published).
[63] J. Fukuda, M. Yoneya, and H. Yokoyama, Eur. Phys. J. E **13**, 87 (2004).
[64] D. Andrienko, M. P. Allen, G. Skačej, and S. Žumer, Phys. Rev. E **65**, 041702 (2002).
[65] S. Grollau, N. L. Abbott, and J.J. de Pablo, Phys. Rev. E **67**, 011702 (2003).
[66] O. Guzmán, E. B. Kim, S. Grollau, N. L. Abbott, and J. J. de Pablo, Phys. Rev. Lett. **91**, 235507 (2003).
[67] P. M. Morse and H. Feshbach, *Methods of Theoretical Physics* (McGraw-Hill, New York, 1953).
[68] J.-R. Roan and T. Kawakatsu, J. Chem. Phys. **116**, 7283 (2002).
[69] W. H. Press, S. A. Teukolsky, W. T. Vetterling, and B. P. Flannery, *Numerical Recipes in C*, 2nd ed. (Cambridge University Press, Cambridge, 1992).
[70] P. C. Hohenberg and B. I. Halperin, Rev. Mod. Phys. **49**, 435 (1977).
[71] J. Fukuda and H. Yokoyama, Phys. Rev. E **66**, 012703 (2002).
[72] P. D. Olmsted and P. Goldbart, Phys. Rev. A **46**, 4966 (1992).
[73] The derivative $d\overline{F}/dD$ is calculated numerically using the following formula: $d\overline{F}(D)/dD=(\Delta D_1+\Delta D_2)^{-1}[(\Delta D_2/\Delta D_1)\overline{F}(D+\Delta D_1)+(\Delta D_1/\Delta D_2-\Delta D_2/\Delta D_1)\overline{F}(D)-(\Delta D_1/\Delta D_2)\overline{F}(D-\Delta D_2)]+O(\Delta D^2)$. Here $\Delta D_1, \Delta D_2 > 0$.